



ELSEVIER



C. R. Physique ●● (●●●●) ●●●-●●●



COMPTES RENDUS

PHYSIQUE

http://france.elsevier.com/direct/COMREN/

Optical techniques for direct imaging of exoplanets/Techniques optiques pour l'imagerie directe
des exoplanètes

Optical performance of the New Worlds Occulter

Jonathan W. Arenberg^{a,*}, Amy S. Lo^a, Tiffany M. Glassman^a, Webster Cash^b

^a Northrop Grumman Space Technology, One Space Park Drive, Redondo Beach, CA 90278, USA

^b University of Colorado, Department of Astronomy, Boulder, CO 80309, USA

Abstract

The New Worlds Observer (NWO) is a multiple spacecraft mission that is capable of detecting and characterizing extra-solar planets and planetary systems. NWO consists of an external occulter and a generic space telescope, flying in tandem. The external occulter has specific requirements on its shape and size, while the telescope needs no special modification beyond that required to do high-quality astrophysical observations. The occulter is a petal-shaped, opaque screen that creates a high-suppression shadow large enough to accommodate the telescope. This article reports on the optical performance of the novel New Worlds occulter design. It also introduces two new aspects of its optical performance which enhance the detectability of extra-solar planets. We also include a brief discussion of the buildability and the tolerances of the occulter. It is also shown that an occulter design can be found for any set of science requirements. We show that NWO is a viable mission concept for the study of extra-solar planets.

To cite this article: J.W. Arenberg et al., C. R. Physique ●● (●●●●).

© 2007 Académie des sciences. Published by Elsevier Masson SAS. All rights reserved.

Résumé

Performance optique de l'occulteur du NWO. Le projet présenté, New Worlds Observer (NWO) est une mission à deux vaisseaux spatiaux capable de détecter et de caractériser les exoplanètes et les systèmes planétaires. NWO se compose d'un écran opaque externe (occulteur) et d'un télescope classique volant en tandem. L'occulteur doit avoir une forme et une taille particulières, alors que le télescope n'a besoin d'aucune modification spéciale, si ce n'est que de convenir à des observations astrophysiques de haute qualité. L'occulteur, en forme de pétales, réalise une zone d'ombre de haute suppression du flux stellaire, suffisamment étendue pour y loger le télescope. Cet article rend compte des performances optiques de la nouvelle conception d'occulteurs pour NWO et présente deux nouveaux aspects de ses performances optiques qui augmentent la détectabilité des exoplanètes ainsi qu'une brève discussion de la faisabilité et des tolérances de réalisation de l'occulteur. Nous montrons qu'il est toujours possible de définir une forme d'écran adapté à un ensemble d'objectifs scientifiques et prouvons que NWO est un concept viable de mission pour l'étude des exoplanètes. *Pour citer cet article :* J.W. Arenberg et al., C. R. Physique ●● (●●●●).

© 2007 Académie des sciences. Published by Elsevier Masson SAS. All rights reserved.

Keywords: Occulter; Exoplanet detection; New Worlds Observer; Tolerance; Contrast ratio; Inner working angle

Mots-clés : Occulteur ; Détection des exoplanètes ; New Worlds Observer ; Tolérance ; Rapport de contrast

* Corresponding author.

E-mail address: jon.arenberg@ngc.com (J.W. Arenberg).

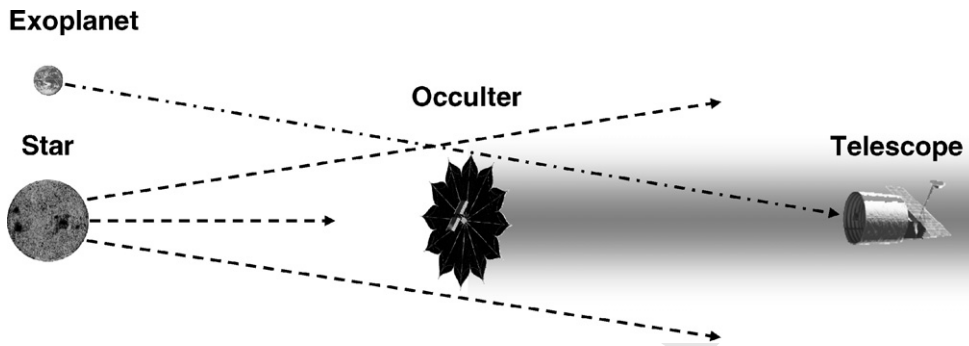


Fig. 1. The basic architecture of the NWO mission. A generic telescope is used in conjunction with the NWO occulter to block out the on-axis starlight and detect and characterize an off-axis source—the extra-solar planet.

1. Introduction

New Worlds Observer (NWO) is a recently introduced mission designed to identify extra-solar planets [1,2]. NWO consists of a telescope and an external occulter aligned with a target star. We currently envision that NWO will orbit the Second Sun–Earth Lagrange point (L2) in a halo orbit. A sketch of the NWO architecture is shown in Fig. 1.

The problem of detecting and, in particular, characterizing an extra-solar planet is pernicious. In the optical region, planets are seen by reflected starlight; the small size and relatively low albedo of the planet means that a brightness difference of $\sim 10^{10}$ exists between the star and planet. In addition, the planet and the star are quite close together; at 10 parsecs away, Earth would be only 100 milliarcseconds (mas) from the Sun. These realities create the performance requirements of the system—we need to be able to achieve a very high contrast ratio, very close to the star. The occulter is capable of creating a given contrast ratio at all angles greater than some minimum, called the Inner Working Angle (IWA). The requirements for the telescope are only that it can detect a faint (~ 30 mag) point source and that it has the resolution necessary to differentiate between two objects ~ 100 mas apart. A 1.5 m telescope has a diffraction limited resolution of 100 mas at $\lambda = 600$ nm and a 3 m telescope would increase the resolution to 50 mas. For NWO, all starlight suppression capabilities are produced by the design of the occulter.

Mission concepts to detect extra-solar planets using an external occulter have a long history [3–7]. However, none of these previous mission concepts were able to demonstrate sufficient starlight suppression for the detection of terrestrial planets. What is novel about NWO is the high-performance, binary occulter [8]. This breakthrough in starlight suppression enables the design of a practical mission to observe extra-solar terrestrial planets. The New Worlds occulter is fully opaque and has a distinctive flower-petal shape that produces destructive interference of on-axis light and virtually no suppression outside of the IWA. Since the star light is extinguished but the target planets are unattenuated, the entire extra-solar system can be observed from the IWA out to the edge of the field of view of the telescope. By having no outer view restrictions, background objects and field stars are simultaneously in view, enabling accurate astrometry to determine the precise location of the planet relative to its parent star.

In this article, we first discuss the basics of the occulter design and describe the simulation we used to model its performance. We describe some key results of this simulation and what it tells us about our tolerance for various types of occulter errors. Finally, we discuss the factors that constrain the specific design of the occulter.

2. Occulter basics

In a recent paper it was shown [8] that an occulter with an offset hypergaussian apodization profile, as shown in Fig. 2, provides a deep, broadband null for on axis light and high transmission for an off axis source. The explicit formulation of this family of solutions is given by:

$$A(\rho) = \begin{cases} 0, & \rho < a \\ 1 - \exp\left[-\left(\frac{\rho - a}{b}\right)^n\right], & \rho > a \end{cases} \quad (1)$$

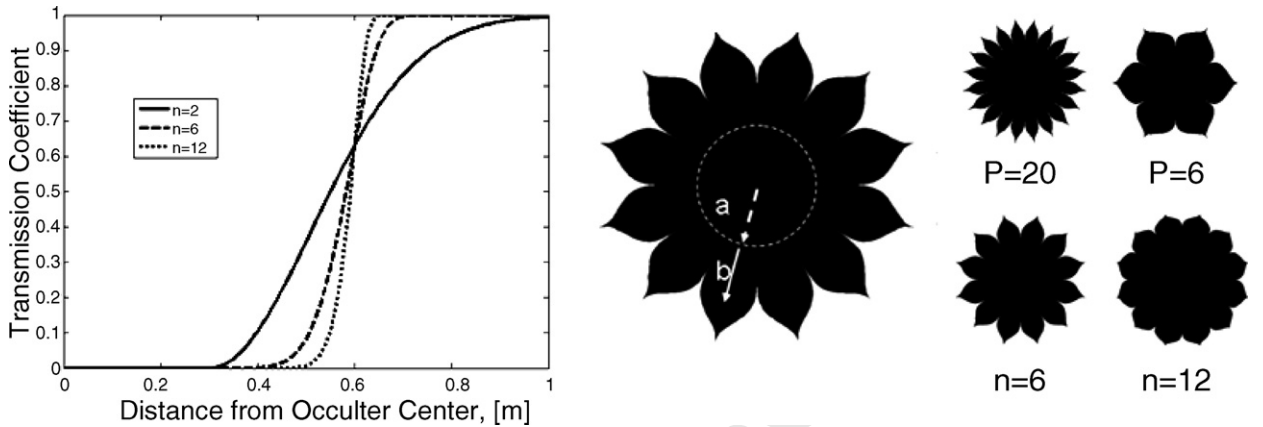


Fig. 2. Left: The apodization function, $A(\rho)$ for the NWO occulter, showing several hypergaussian orders. Center: A 12 petaled occulter with $n = 6$. Right: Illustrations of shapes with different petal numbers and values of n .

where $A(\rho)$ is the apodization (starlight transmission) as a function of radial distance, ρ , from the occulter center. a is the radius of the inner solid disk, b is the $1/e$ length of the hypergaussian function, and n is the order of the hypergaussian.

The fractional intensity, C , of on-axis starlight that remains behind the occulter is:

$$C = \left[n! \left(\frac{\lambda F}{ab} \right)^n \right]^2 \quad (2)$$

where F is the occulter to telescope separation [8]. This simple and elegant result captures the basic performance and scaling of the occulter. A key property of the New Worlds occulter is that if the occulter is designed for a given wavelength, λ , there is greater suppression, at all shorter wavelengths. Eq. (2) also shows that for a given total size ($a + b$), the best performance is obtained when a and b are equal. Eq. (2) can be interpreted as relating the reciprocal of the n th power of the occulter Fresnel number, $(a + b)^2/(\lambda F)$, to the extinction of starlight, and leads to the understanding that the occulter operates in the optical near field, namely in the Fresnel regime.

To generalize this concept from 1 to 2 dimensions [9], we spread out the apodization among a number of petals, P . The occulter is a binary mask with flower-like petals that are completely opaque. Each petal provides a fraction, $T(\rho)$, of the total transmission of the mask:

$$T(\rho) = \frac{2\pi}{P} [1 - A(\rho)] \quad (3)$$

Between radii 0 and a , the screen is completely opaque. For radii larger than a , opaque portions are given by azimuthal angles, θ , within the following limits:

$$\theta_1 = \bigcup_{q=0}^{P-1} \left[\frac{2\pi q}{P} + \frac{T(\rho)}{2} \right] \quad \text{and} \quad \theta_2 = \bigcup_{q=0}^{P-1} \left[\frac{2\pi(q+1)}{P} - \frac{T(\rho)}{2} \right] \quad (4)$$

3. Occulter performance

In order to model the optical performance of the occulter, we must solve the Fresnel integral:

$$U(x_o, y_o) = \frac{\exp(ikF)}{iF\lambda} \iint_A U(x_1, y_1) \exp \left\{ \frac{ik}{2F} [(x_o - x_1)^2 + (y_o - y_1)^2] \right\} dx_1 dy_1 \quad (5)$$

where subscripts 1 indicate the occulter plane and subscripts 0 indicate the telescope aperture plane. The shadow of the occulter is the output of this model. Fig. 3 shows examples of the modeled occulter shadow for several different

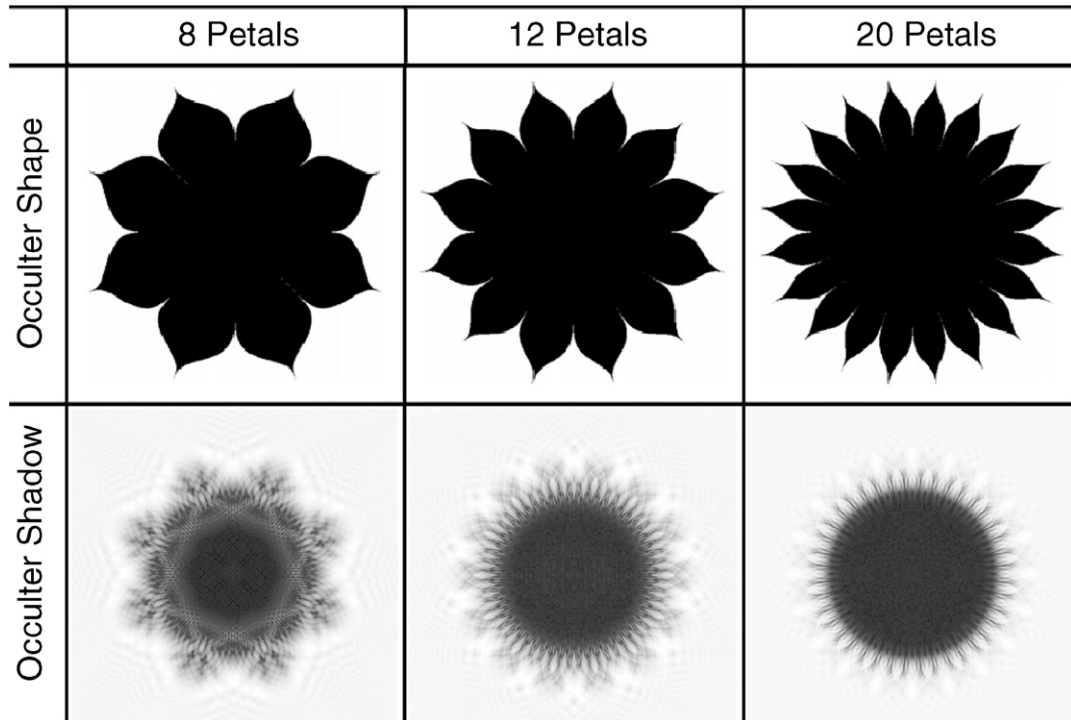


Fig. 3. The shadow created by the NWO occulter for various numbers of petals. The telescope is flown within the central, dark portion of this shadow.

petal numbers. Fig. 3 illustrates the role of the number of petals in shaping the shadow. It can be seen in Fig. 3 that the shadow is smoother for the case of 20 petals that it is for the 8 and 12 petal case. In Fig. 4 we show that the shadow is larger and darker at shorter wavelengths for a given occulter design and F . Thus, occulter designs are driven by the longest wavelength required.

The telescope aperture sits in the center of the occulter's shadow and collects the residual light from the star and forms an image at its focal plane. To understand the properties of such an image, the residual light field at the telescope aperture is calculated from Eq. (5) and then taken to the telescope focal plane via a Fourier transform. This resulting image is the PSF of the occulter. Fig. 5 shows the result of such an analysis for an on-axis source and a 12 petal occulter. In the left panel of Fig. 5, the twelve fold symmetry of the occulter PSF is evidenced. It is also clear that the on-axis source is not only strongly attenuated, but the residual light is defocused over a large area resulting in additional attenuation.

To add the planet light to the simulation, we create an input distribution consisting of two sets of plane waves: a bright, on-axis source with flat phase fronts and a dim, off-axis source with a small tilt to its phase fronts. The results of this simulation show that the occulter has another exiting property; the on-axis light is defocused and the off-axis light is not. The residual starlight is spread out over an area roughly corresponding to the IWA, while the off-axis planet light remains concentrated, increasing the contrast between the on-axis and off-axis sources. This additional factor allows the system to detect planets about two orders of magnitude fainter than the simple suppression factor, C , would indicate (Fig. 6).

Our optical simulation uncovered another property of the NWO occulter useful in planet detection: the petals cause local enhancements of off-axis sources. This result is shown in Fig. 7, where a planet placed behind an occulter petal is preferentially brightened by the diffractive focusing effect of the occulter. As seen in the central images of Fig. 7, it is easier to discern the planet signal when the object is situated behind a petal. At larger offsets this effect becomes less pronounced, as seen in the rightmost images in Fig. 7. A corollary to this discovery is that if a planet is located near the tips of the petals, there is up to a factor of 2 brightening in the planet intensity, relative to the intensity far off axis. This effect will improve the signal to noise ratio of the detection.

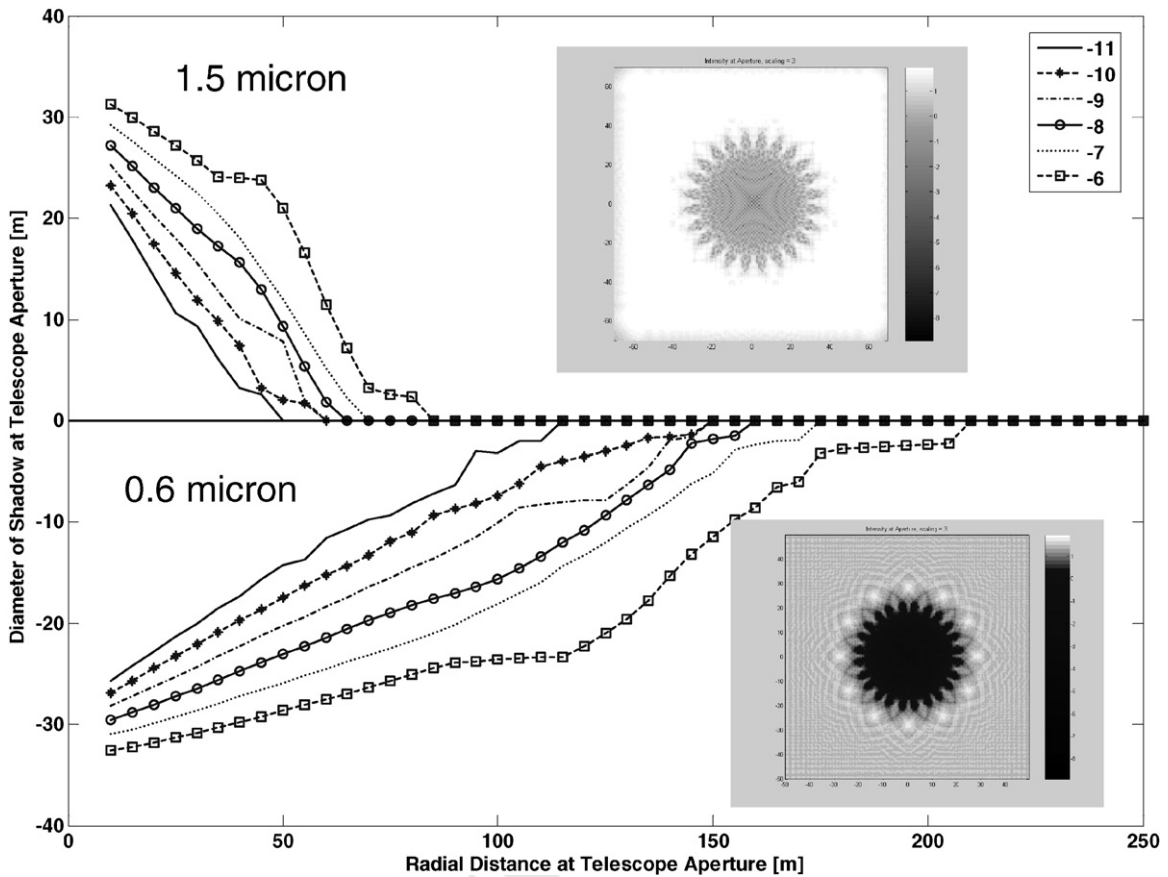


Fig. 4. The anatomy of the occulter shadow. The diameter of the shadow is plotted as a function of distance behind the occulter. Note that the x -axis is in units of Mm, or 10^6 m. The different lines show the shadow diameter for different contrast ratios. The insets give notional pictures of what the different shadows look like in 2-D.

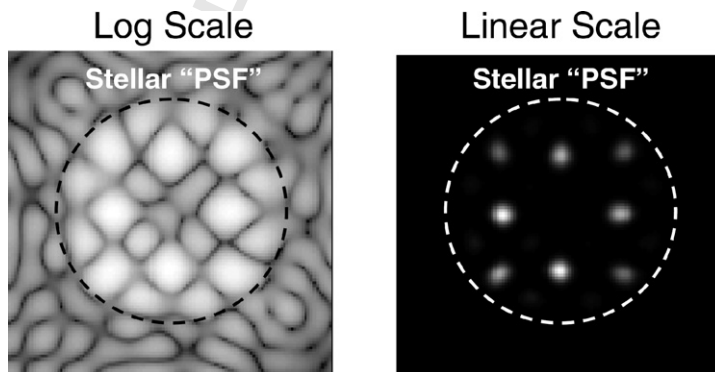


Fig. 5. Simulations of the occulter performance show that the residual light of the occulted star, as seen by the telescope, resembles an out of focus image. On the left is a log scale image of the residual stellar light (the effective PSF of the star), which appears as a bright central blob. On the right is a linear scale image of the same distribution in which only the highest intensity peaks are visible.

4. Occulter tolerance

Now that we have established that the occulter can achieve the desired performance, we turn to the question of how much error in the occulter properties we can tolerate. In order to assure that NWO is buildable, we must prove that the error tolerances are within reasonable limits.

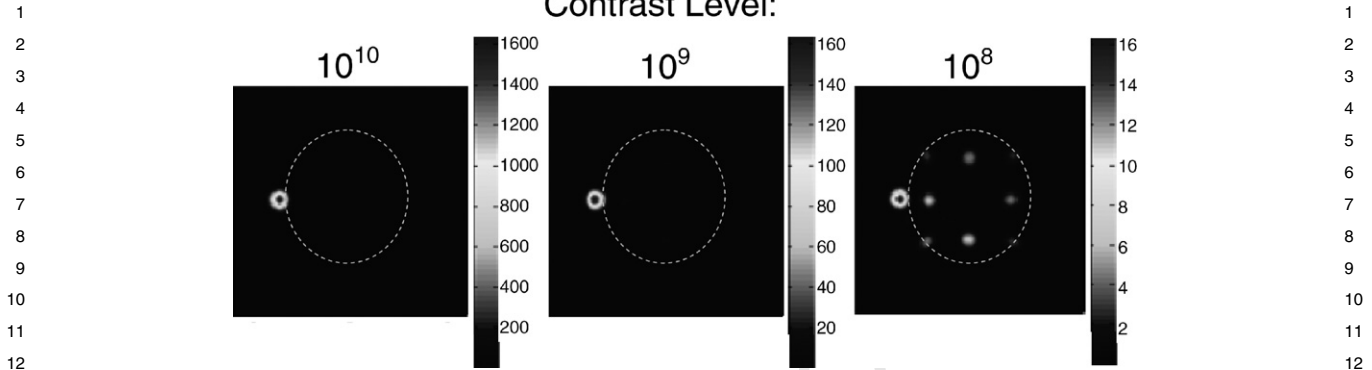


Fig. 6. Inserting a faint, off-axis source into the simulation shows that the occulter only needs to create a 10^8 contrast suppression to effectively detect extra-solar planets that are 10^{10} times fainter than their central star. This is because the starlight is out of focus and distributed over many pixels. The intensity per pixel is therefore much lower than that calculated by suppression alone. The white circle indicates the IWA.

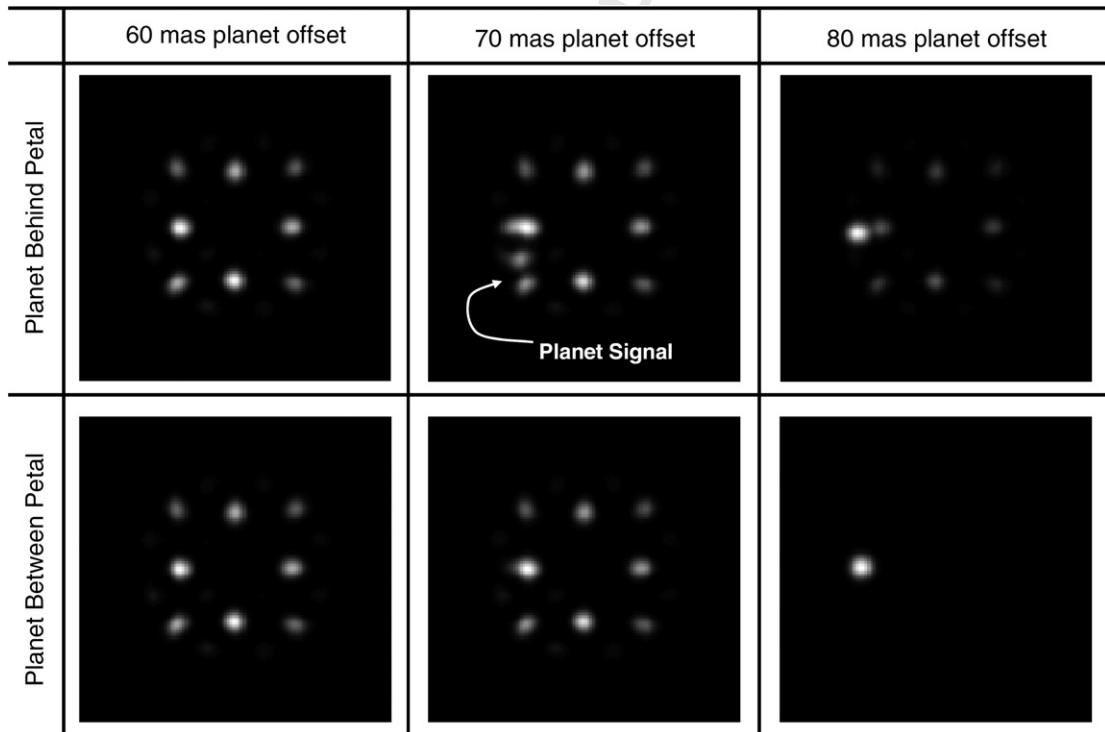


Fig. 7. The location of the planet with respect to the occulter petals affects its focal plane appearance. The top row shows the planet signal as a function of offset from the star in units of mas, where the planet is always ‘behind’ one petal of the occulter. The bottom row shows the same, but with the planet always ‘between’ two occulter petals. Planets located behind a petal receive an enhancement from the diffractive focusing effects of the apodized petals. The geometric IWA of the occulter simulated here is 85 mas.

Specific values for the occulter tolerances will be the result of a rigorous derivation including all sources of performance degradation [10]. If, for simplicity, all sources of error besides the occulter are ignored and a single point design (fixed n , λ , a , b , and F) is adopted, the scale of the tolerances can be derived from a perturbation analysis [8]. Table 1 summarizes the tolerances of the occulter.

The positional tolerance of the occulter is the alignment tolerance between the telescope and the occulter and is based on the size of the high-contrast shadow. A larger occulter has a larger shadow, therefore this positional tolerance

Table 1
The acceptable tolerances for various types of errors in the occulter

Tolerance	Category	Value
Position	Lateral	Several meters
	Axial	100s km
Angle	Rotation	Any rotation
	Pitch/yaw	Many degrees
Shape	Truncation	1 mm
	Scale	10%
Hole	Edge errors	3 cm ²
	Single hole	3 cm ²
	Pinholes	Total area <3 cm ²

is dependent on occulter size. A conservative estimate for the size of the zone that the telescope must stay in is approximately 5 meters in diameter for a 25 m occulter at a distance of 30 000 km. The axial tolerance is much looser.

The occulter is rotationally symmetric, and therefore tolerates any angular rotation about its center. The face-on tilt of the occulter, however, will change the projected shape and eventually destroy the interference symmetry produced by the petals. We estimate that this tilt, or pitch/yaw angle tolerance, is on the order of 10 to 15 degrees [8].

Shape tolerance is basically the deployment and manufacturing errors. These can be described with (i) an RMS value, which indicates how large the deviation from the ideal shape the actual petal is, and also by (ii) the frequency of the deviation. These errors describe how well the manufacturing process comes to producing the ideal shape of the petals. Of particular concern is the ability to produce the petal tips. In principle, the petal tips extend to infinity. In practice, the petal tips must be truncated at a reasonable point so that they are deployable. To first order, our simulations indicate that petal tips can be truncated to 1 mm width without significantly affecting the performance (see Section 5).

We performed shape tolerance analysis of the occulter by doing a one-dimensional simulation of the achievable contrast ratio by using a perturbed apodization function. The perturbations on the apodization function are directly related to shape perturbations on the occulter. The perturbation to the transmission function, T , is related to the actual deviation, δw_o , on the petal by the following:

$$\delta T(\rho) = \frac{\delta w_o \sin(\nu\rho)}{2\pi\rho} \quad (6)$$

where ν is the spatial frequency of the perturbation.

The central and right portions of Fig. 8 show the effect of various amplitudes and frequencies of error on a 25 m occulter designed to operate at a maximum wavelength of 800 nm. Shown in Fig. 8 on the left side with the dashed line is the original, unperturbed apodization function. The solid line is the perturbed apodization function, where a very large perturbation was inserted for illustrative purposes. The high-frequency variations have a smaller impact for a given δw_o than the low-frequency variations. This is due to the fact that the higher-frequency errors will have more oscillations in a given Fresnel zone, and therefore degrade the balance of the Fresnel zones of the ideal figure less than errors that oscillate slower.

5. Occulter design space topology

In this section, we investigate the design space of the occulter, i.e. the values of occulter diameter, D , and occulter-telescope separation, F , required to meet the performance goals. The key requirements that must be simultaneously satisfied are sufficient starlight suppression, S , and small IWA.

From our modeling we know that the starlight suppression, S , is proportional to the on axis contrast ratio, C :

$$S = \kappa(D_T, \sigma, T, \lambda, F, a, b, n) \left[n! \left(\frac{\lambda F}{ab} \right)^n \right]^2 \quad (7)$$

The constant of proportionality κ , is a function of the telescope diameter, D_T , the misalignment of the telescope to occulter, σ , the tolerances on the occulter, T , and the parameters of the occulter (λ, F, a, b, n). For a given set of parameters, κ can be calculated using the Fourier transform methods discussed in Section 3.

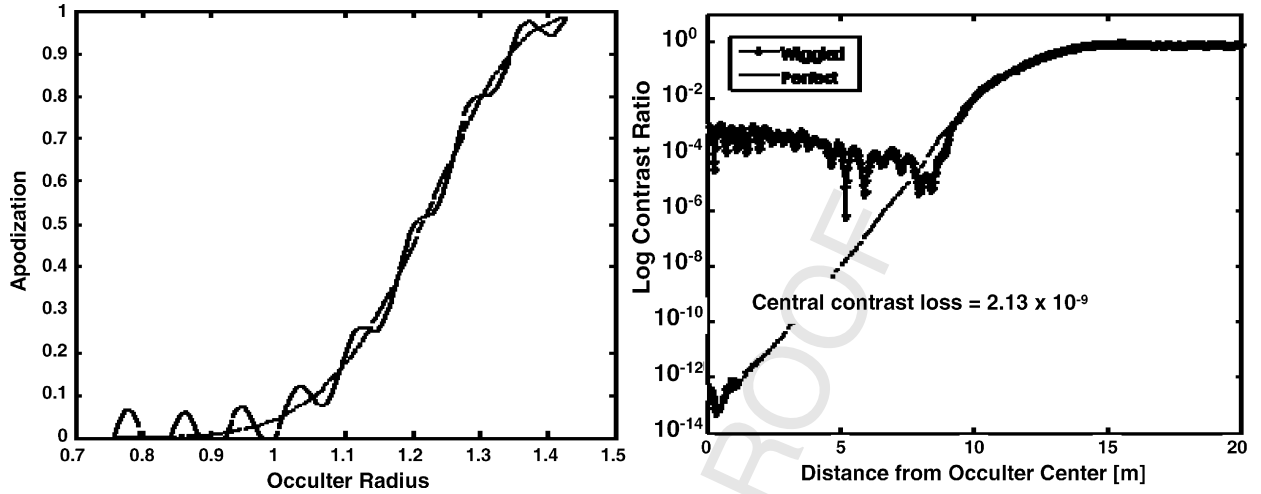


Fig. 8. The perturbed apodization (left) and the resulting contrast loss (right). We have inserted a very large perturbation. Dashed lines indicate the ideal apodization, and the solid lines indicated the perturbed or ‘wiggled’ apodization.

In creating a realistic occulter design, the mathematical apodization function, $A(\rho)$ which extends to infinity, must be truncated at a finite length. We have found that the best means for describing the truncation is the width of the petal at its end. Furthermore, if this truncated petal width is less than a few mm, there is negligible degradation in contrast or suppression. If the allowed truncation width is denoted τ , then:

$$\tau = \frac{2\pi a}{P} \exp\left[-\left(\frac{r_o - a}{b}\right)^n\right] \quad (8)$$

Eq. (8) can be solved for the occulter radius, r_o . Recalling that the best occulter performance is realized when $a = b$ we get:

$$r_o = \left\{ \left[\ln\left(\frac{2\pi a}{\tau P}\right) \right]^{1/n} + 1 \right\} a \quad (9)$$

Eq. (9) gives an expression for the radius of the outer edge of the petal, which is a conservative estimate of the geometric IWA. It should be noted that once P , τ , a , and n are selected, the natural logarithmic term is a constant and (9) can be expressed as:

$$r_o = (Q + 1)a \quad (10)$$

The geometric IWA, IWA_G , is given in radians by:

$$IWA_G = \frac{r_o}{F} \quad (11)$$

The occulter is oriented so that the side facing the telescope is away from the sun. This places the occulter in an edge on orientation of the sun. Sunlight scattering off the edge of the occulter will increase the effective IWA. Controlling this edge scatter is one of the design requirements for the occulter, however, while this edge scatter can be small, some pixels on the sunlit side of the occulter may have a local magnitude at or above the required suppression limit. This locally increases the IWA by a few pixels. The angular extent of the increase in IWA, Γ , is the angular extent of the light that is above the suppression requirement, S_{req} . Γ is proportional to the angular extent of the telescope point spread function (PSF). The scaling factor, g , is dependent on the brightness of the edge, B_{edge} , the suppression requirement, and the pixel angular subtense, α :

$$\Gamma = g(B_{edge}, S_{req}, \alpha)PSF \quad (12)$$

All of the parameters in Eq. (12) are known once an occulter design is selected. S_{req} and α are fixed and the edge brightness will scale with $1/F^2$, so Γ can be expressed as:

$$\Gamma = \frac{h}{F^2} \quad (13)$$

where h is a constant whose value is determined by the specific system.

The complete expression for IWA is:

$$IWA = IWA_G + \Gamma \tag{14}$$

Substitution of (13) into (14) gives the final expression for IWA as:

$$IWA = \frac{r_o}{F} + \frac{h}{F^2} \tag{15}$$

For the New Worlds occulter to be a viable mission concept, it must be shown that there is a reasonable occulter design for any IWA and S requirements. To make this demonstration, Eqs. (7) and (15) must be solved together for a and this solution must be shown to exist and be well behaved. The system of Eqs. (7) and (15) has the solution:

$$a_{\min} = \left[\frac{\lambda(Q+1)}{IWA - \frac{h}{F^2}} \right] \left(\frac{\kappa}{S} \right)^{1/2n} (n!)^{1/n} \tag{16}$$

Examination of Eq. (16) brings insight into the nature of the allowed design space. First, a value for a minimum value of a , a_{\min} , can always be found. This clearly demonstrates that there is a solution for any pair of IWA and S requirements. Second, the requirements for IWA and S are not antagonistic, meaning both appear on the same side of the fraction in (16) and compensation for increase in one requirement does not come at the expense of the other. Since the IWA and S both appear in the denominator of the expression, deeper shadows and decreased IWAs are *both* met with increasing the value a , i.e. increasing the occulter size.

Fig. 9 shows a notional diagram of the occulter design space which meets the IWA and suppression requirements. Their exact values do not matter, as the topology of this diagram is general to any IWA and suppression values of interest for planet observation. The dark regions are occulter designs that do not meet our given suppression and IWA requirements and the light regions are those that do meet these requirements.

The superimposed shaded regions indicate the effects of technological constraints on the occulter design space. Existing technology and launch mass limits place constraints on the size of the occulter that can be built. There is also a separation constraint in order to allow the occulter to be moved to cover sufficiently many targets to constitute a feasible planet-finding campaign. The effects of shape, alignment, and sunlight scattering errors all lead to a need for a larger, more distant occulter, as discussed above.

Our main conclusion is that there is *always* an occulter that can meet a given set of suppression and IWA requirements. The occulter can therefore be scaled for any extra-solar planet mission—terrestrial or giant planets. Furthermore, higher suppression and smaller IWA can be achieved by building a larger occulter and placing it at farther away from the telescope, providing a means to compensate for any errors. The building of margin against one criterion is not done at the expense of the other.

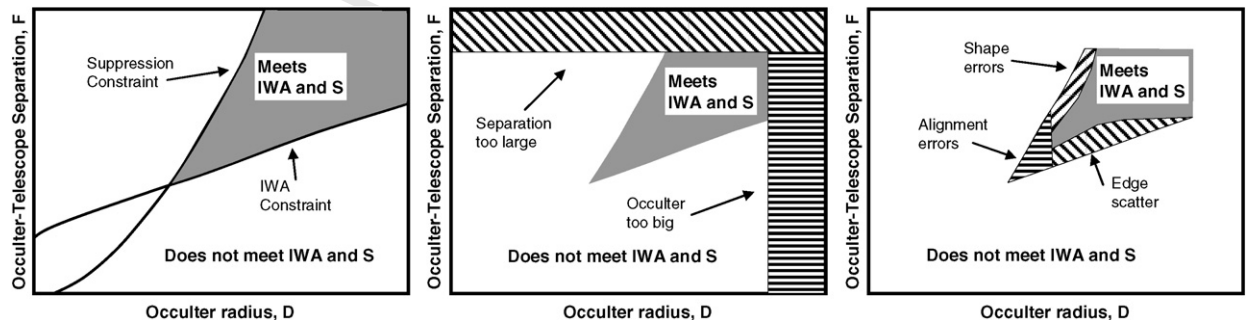


Fig. 9. The notional occulter design space. The light gray area indicates the occulter designs with radii and separations capable of producing a certain IWA and suppression requirement. The dark areas do not. The shaded regions correspond to different effects that constrain the design space.

6. Conclusion

The optical performance of the NWO occulter has been presented, along with how that performance scales with the various design parameters. Our occulter is different from previous occulters due to its binary transmission and hypergaussian shape, allowing exceptional suppression performance. The New Worlds occulter also has some additional properties reported here for the first time. The first of these new properties is the defocus of the on-axis source relative to the off-axis source, affording additional suppression. The second newly reported property is an enhancement of the off-axis source depending on its azimuth if it is located within the IWA and outside the central obscuration.

We also discussed the engineering issues surrounding the buildability of the occulter. We presented first order estimates of these tolerances, which indicate no major problems with constructing the NWO design. Finally, we have demonstrated that design solutions always exist to meet given science requirements. On the basis of these results, we conclude that the New Worlds Observer is a flexible and feasible technology for extra-solar planet finding missions.

It should be noted that the New Worlds Observer is very much a work in progress. Progress to date has been rapid, the interested reader is invited to contact the authors to obtain the latest results. We look forward to sharing our progress.

Acknowledgements

The work of the Northrop Grumman employees has been supported on internal funding. We are extremely grateful for the support. W. Cash is supported through a grant from the NASA Institute for Advanced Concepts.

References

- [1] W. Cash, J. Kasdin, S. Seager, J. Arenberg, Direct studies of exo-planets with the New Worlds Observer, *Proc. SPIE* 5899 (2005) 274–284.
- [2] J. Arenberg, W. Cash, New Worlds Observer: A novel mission concept for exoplanetary studies, *Proc. IAU Colloq.* 200 (2006) 199–204.
- [3] L. Spitzer, The beginnings and future of space astronomy, *Amer. Scientist* 50 (1962) 473–484.
- [4] C. Marchal, Concept of a space telescope able to see the planets and even the satellites around the nearest stars, *Acta Astron.* 12 (1985) 195–201.
- [5] F. Cocks, J. Bischoff, S. Watkins, K. Higuchi, P. Bely, Extrasolar planetary detection via stellar occultation: a novel “smaller, cheaper, faster” concept employing the Hubble Space Telescope, *Proc. SPIE* 2807 (1996) 74–85.
- [6] C.J. Copi, G. Starkman, The Big Occulting Steerable Satellite (BOSS), *Astrophys. J.* 532 (2000) 581–592.
- [7] I. Jordan, et al., Apodized square aperture plus occulter concept for TPF, *Proc. SPIE* 5487 (2004) 1391–1401.
- [8] W. Cash, Detection of Earth-like planets around nearby stars using a petal-shaped occulter, *Nature* 442 (2006) 51–53.
- [9] R. Vanderbei, D. Spergel, J. Kasdin, Circularly symmetric apodization via star-shaped masks, *Astrophys. J.* 599 (2003) 686–694.
- [10] J. Arenberg, A. Lo, W. Cash, R. Polidan, New Worlds Occulter performance: a first look, *Proc. SPIE* 6265 (2006) 62651W1–62651W14.